Joint 48th IEEE Conference on Decision and Control and
28th Chinese Control Conference
Shanghai, P.R. China, December 16-18, 2009

Sliding-mode real-time mobile platform control in the presence of uncertainties

Razvan Solea, Adrian Filipescu and Grigore Stamatescu

Abstract— **In this paper, a new sliding-mode trajectory-tracking wheeled mobile robots (WMR) control is proposed. Dynamic model with uncertainties parameters (unknown or time varying mass and moment of inertia) of the WMR is taken into account. Robust stability depending on upper bound uncertainties, is guaranteed. A mobile platform, PatrolBot, with two driving wheels and two rear wheels is used in order to check proposed sliding-mode control. Closed-loop real-time control results are supplied. Good trajectory-tracking performances (small position and orientation errors) in the presence of external disturbances are obtained.**

I. INTRODUCTION

The development of robotic systems with increasing degree of autonomy is at, present, a challenging issue in robotic research. In particular, wheeled mobile robots (WMR) are being given much attention in recent literature mainly because of their wide spectrum of practical application. In fact, WMR are extensively used in several fields where transportation, inspection and operation tasks are required (industry, assembly, mining, safety).

Another promising application is the design of robotic systems for the assistance of disabled, handicapped or elderly people. As is well known, three major problems have been addressed in control design for WMR, namely trajectory tracking, path following and point stabilization.

WMR is one of the well-known system with nonholonomic constraints and it contains a class of mechanical systems characterized by kinematic constraints that are not integrable and cannot therefore be eliminated from the model equations. From Brockett's necessary conditions for stability, one may demonstrate that systems with nonintegrable velocity constraints cannot be stabilized to a point with smooth static-state feedback [1], [2]. With this result, the control problems of the nonholonomic system become a challenge task. In the early researches, the controller for kinematic model was concentrated on [3], [4], [5]. The control input of the controller for kinematic model is generally velocity, but it is more realistic that the real input is torque. There are many researches on torque controller for the dynamic model in recent years [6], [7]. However, these torque controllers can not show high performance in practical wheeled robot system because we can't obtain all precise parameters of a wheeled mobile robot.

In this article, the trajectory tracking problem for a mobile robot in the presence of uncertainties has been solved by means of a sliding mode control law based on the WMR dynamic model.

The proposed control policy is based on two nonlinear sliding surfaces ensuring the tracking of the three output variables exploiting the nonholonomic constraint. When a sliding motion occurs on these surfaces, the position errors are forced to zero in the reduced order system with assigned dynamics. This in turn implies the vanishing of the orientation error on the second surface.

II. WHEELED MOBILE ROBOT DYNAMIC MODEL

A large class of mechanical nonholonomic systems is described by the following form of dynamic equations based on Euler Lagrange formulation [8]:

$$M(q)\cdot\ddot{q}+C(q,\dot{q})\cdot\dot{q}+G(q)=B(q)\cdot\tau+J^T(q)\cdot\lambda. \quad (1)$$

While the nonholonomic constraint is

$$J(q)\cdot\dot{q}=0 \quad (2)$$

where q is the n dimensional vector of configuration variables, $M(q)$ is a symmetric positive definite $n\times n$ matrix, $C(q,\dot{q})$ presents the n vector of centripetal and coriolis torques, $G(q)$ is the n vector of gravitational torques, $B(q)$ is the $n\times r$ input transformation matrix $(r<n)$, τ is the r dimensional vector of inputs and λ the Lagrange multipliers of constrained forces.

A simple structure of differential drive mobile robot is shown in Fig 1. Two independent analogous DC motors are the actuators of left and right wheels, while two free wheel casters are used to keep the platform stable.

Pose vector of robot in the surface is defined as $q=(x_r,y_r,\theta_r)$ where x_r and y_r are the coordinates of point CG; center of axis of wheels, and θ_r is the orientation angle of robot in the inertial frame. One can write the dynamic equations of mobile robot according to (1), using the fact that $G(q)$ and $C(q,\dot{q})$ are zero.

$$\begin{bmatrix} m & 0 & 0\\ 0 & m & 0\\ 0 & 0 & I\end{bmatrix}\cdot\begin{bmatrix}\ddot{x}_r\\ \ddot{y}_r\\ \ddot{\theta}_r\end{bmatrix}=$$
$$=\tfrac{1}{R}\cdot\begin{bmatrix} cos\theta_r & cos\theta_r\\ sin\theta_r & sin\theta_r\\ L & -L\end{bmatrix}\cdot\begin{bmatrix}\tau_r\\ \tau_l\end{bmatrix}+\begin{bmatrix} sin\theta_r\\ -cos\theta_r\\ 0\end{bmatrix}\cdot\lambda \quad (3)$$

This work was supported by the Romanian High Education Scientific Research National Council, under project IDEAS, ID 641.

R. Solea and A. Filipescu are with the Department of Automation and Industrial Informatics, Universy "Dunarea de Jos" of Galati, 111 Domneasca, 800201 Galati, Romania razvan.solea@ugal.ro adrian.filipescu@ugal.ro

G. Stamatescu is MSc student in Control Systems, Faculty of Automation and Computers, Polytechnic University of Bucharest, Romania gorrocs@gmail.com

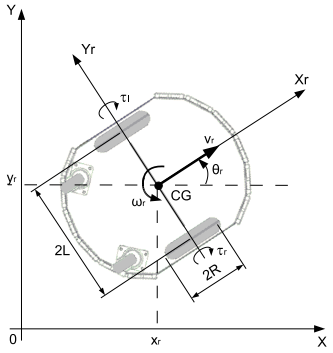

Fig. 1. Definition of configuration variables of mobile robot.

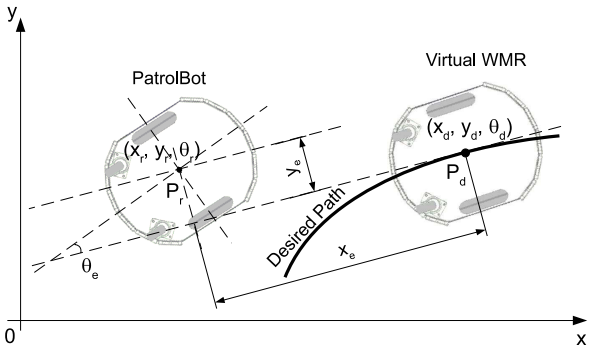

Fig. 2. Lateral, longitudinal and orientation errors (trajectory-tracking).

and

$$\lambda = -m \cdot (\dot{x}_r \cdot cos\theta_r + \dot{y}_r \cdot sin\theta_r) \cdot \dot{\theta}_r. \tag{4}$$

Where τ_r and τ_l are the torques of right and left motors, m and I present the mass and inertia of robot respectively. R is the radius of wheels and $2 \cdot L$ is the distance of rear wheels.

The nonholonomic constraint, the no slip condition, is written in the form of (2):

$$\dot{x}_r \cdot sin\theta_r - \dot{y}_r \cdot cos\theta_r = 0. \tag{5}$$

This equation is not integrable, so the feasible trajectory of robot is limited.

Assuming $u_1 = \tau_r + \tau_l$ and $u_2 = \tau_r - \tau_l$ (3) becomes:

$$\begin{aligned} m \cdot \ddot{x}_r &= -m \cdot \dot{y}_r \cdot \dot{\theta}_r + \frac{u_1}{R} \cdot cos\theta_r, \\ m \cdot \ddot{y}_r &= m \cdot \dot{x}_r \cdot \dot{\theta}_r + \frac{u_1}{R} \cdot sin\theta_r, \\ I \cdot \ddot{\theta}_r &= \frac{L}{R} \cdot u_2. \end{aligned} \tag{6}$$

Equation (6) can be rewritten like

$$\begin{aligned} \ddot{x}_r &= -\dot{y}_r \cdot \dot{\theta}_r + \alpha \cdot u_1 \cdot cos\theta_r, \\ \ddot{y}_r &= \dot{x}_r \cdot \dot{\theta}_r + \alpha \cdot u_1 \cdot sin\theta_r, \\ \ddot{\theta}_r &= \beta \cdot u_2. \end{aligned} \tag{7}$$

The real mass of the WMR is supposed to be uniformly distributed all the time and to be time-varying with bounded uncertainty with known nominal mass. Due to the time-varying mass, the moment of inertia becomes time-depending with bounded uncertainty.

The real values of the parameters

$$\alpha(t) = \frac{1}{R \cdot m(t)}, \quad \beta(t) = \frac{L}{R \cdot I(t)} \tag{8}$$

are time varying with upper bounded uncertainties

$$\begin{aligned} \alpha_{real}(t) &= \alpha_{nom} + \Delta\alpha(t);\ |\Delta\alpha| \leq \Delta\alpha_{max}, \\ \beta_{real}(t) &= \beta_{nom} + \Delta\beta(t);\ |\Delta\beta| \leq \Delta\beta_{max}. \end{aligned} \tag{9}$$

Known the kinematic relationship

$$\dot{q} = \begin{bmatrix} cos\theta_r & 0 \\ sin\theta_r & 0 \\ 0 & 1 \end{bmatrix} \cdot \begin{bmatrix} v_r \\ \omega_r \end{bmatrix} \tag{10}$$

Differentiating (10):

$$\ddot{q} = \begin{bmatrix} -\dot{\theta}_r \cdot sin\theta_r & 0 \\ \dot{\theta}_r \cdot cos\theta_r & 0 \\ 0 & 1 \end{bmatrix} \cdot \begin{bmatrix} v_r \\ \omega_r \end{bmatrix} + \begin{bmatrix} cos\theta_r & 0 \\ sin\theta_r & 0 \\ 0 & 1 \end{bmatrix} \cdot \begin{bmatrix} \dot{v}_r \\ \dot{\omega}_r \end{bmatrix}. \tag{11}$$

Therefore

$$\begin{aligned} \ddot{x}_r &= -v_r \cdot \dot{\theta}_r \cdot sin\theta_r + \dot{v}_r \cdot cos\theta_r, \\ \ddot{y}_r &= v_r \cdot \dot{\theta}_r \cdot cos\theta_r + \dot{v}_r \cdot sin\theta_r, \\ \ddot{\theta}_r &= \dot{\omega}_r. \end{aligned} \tag{12}$$

Comparing (7) with (12) we can write

$$\begin{aligned} -\dot{y}_r \cdot \dot{\theta}_r + \alpha \cdot u_1 \cdot cos\theta_r &= -v_r \cdot \dot{\theta}_r \cdot sin\theta_r + \dot{v}_r \cdot cos\theta_r, \\ \dot{x}_r \cdot \dot{\theta}_r + \alpha \cdot u_1 \cdot sin\theta_r &= v_r \cdot \dot{\theta}_r \cdot cos\theta_r + \dot{v}_r \cdot sin\theta_r, \\ \beta \cdot u_2 &= \dot{w}_r. \end{aligned} \tag{13}$$

Multiplying the first part of (13) by $cos\theta_r$ and the second part by $sin\theta_r$, and adding the results the following is obtained

$$\dot{v}_r = \frac{u_1}{m \cdot R}, \qquad \dot{\omega}_r = \frac{u_2 \cdot L}{I \cdot R}. \tag{14}$$

Where v and ω are the linear and angular velocities of mobile robot.

III. WMR Mobile Platform Control

The application of SMC strategies in nonlinear systems has received considerable attention in recent years [9]-[14]. A well-studied example of a non-holonomic system is a WMR that is subject to the rolling without slipping constraint.

In the case of trajectory-tracking the path is to be followed under time constraints. The path has an associated velocity profile, with each point of the trajectory embedding spatiotemporal information that is to be satisfied by the WMR along the path. Trajectory tracking is formulated as having the WMR following a virtual target WMR which is assumed to move exactly along the path with specified velocity profile.

A. Trajectory-tracking errors

Without loss of generality, it can be assumed that the desired trajectory $q_d(t) = [x_d(t), y_d(t), \theta_d(t)]^T$ is generated by a virtual unicycle mobile robot (see Fig. 2). The kinematic relationship between the virtual configuration $q_d(t)$ and the corresponding desired velocity inputs $[v_d(t), \omega_d(t)]^T$ are:

$$\begin{bmatrix} \dot{x}_d \\ \dot{y}_d \\ \dot{\theta}_d \end{bmatrix} = \begin{bmatrix} cos\theta_d & 0 \\ sin\theta_d & 0 \\ 0 & 1 \end{bmatrix} \cdot \begin{bmatrix} v_d \\ \omega_d \end{bmatrix}. \quad (15)$$

This trajectory should satisfy not only the kinematic equations but also the nonholonomic constraint:

$$\dot{x}_d \cdot sin\theta_d - \dot{y}_d \cdot cos\theta_d = 0. \quad (16)$$

When a real robot is controlled to move on a desired path it exhibits some tracking error. This tracking error, expressed in terms of the robot coordinate system, as shown in Fig. 2, is given by

$$\begin{bmatrix} x_e \\ y_e \\ \theta_e \end{bmatrix} = \begin{bmatrix} cos\theta_d & sin\theta_d & 0 \\ -sin\theta_d & cos\theta_d & 0 \\ 0 & 0 & 1 \end{bmatrix} \cdot \begin{bmatrix} x_r - x_d \\ y_r - y_d \\ \theta_r - \theta_d \end{bmatrix}. \quad (17)$$

Consequently one gets the error dynamics for trajectory tracking as

$$\begin{cases} \dot{x}_e = \dot{x}_r \cdot cos\theta_d + \dot{y}_r \cdot sin\theta_d + \omega_d \cdot y_e - v_d \\ \dot{y}_e = -\dot{x}_r \cdot sin\theta_d + \dot{y}_r \cdot cos\theta_d - \omega_d \cdot x_e \\ \dot{\theta}_e = \omega_r - \omega_d \end{cases} \quad (18)$$

In this paper it is assumed that $|\theta_e| < \pi/2$.

B. Sliding-mode control

A Sliding Mode Controller is a Variable Structure Controller(VSC). Basically, a VSC includes several different continuous functions that map plant state to a control surface, and the switching among different functions is determined by plant state that is represented by a switching function. Without lost of generality, consider the design of a sliding mode controller for the n^{th}-order:

$$x^{(n)} = f(x,t) + b(x,t) \cdot u \quad (19)$$

where x is the state variable; $x^{(n)} = \left[x, \dot{x}, \ddot{x}, \ldots, x^{(n-1)}\right]^T$; $x^{(n)}$ is the n^{th}-order derivative of x; f is a nonlinear function; b is the gain and u is the control input.

The following is a possible choice of the structure of a sliding mode controller [15]:

$$u = u_{eq} - k \cdot sgn(s) \quad (20)$$

where u_{eq} is equivalent control and can be interpreted as the continuous control law that would maintain $\dot{s} = 0$ if the dynamics were exactly known. s is called switching function because the control action switches its $sign$ on the two sides of the switching surface $s = 0$. s are defined as:

$$\begin{aligned} s_1 &= \dot{x}_e + \gamma_1 \cdot x_e, \\ s_2 &= \dot{\theta}_e + \gamma_2 \cdot \theta_e + \gamma_0 \cdot sgn(\theta_e) \cdot |y_e| \end{aligned} \quad (21)$$

where x_e, y_e and θ_e are define in (16).

$sgn(s)$ is a sign function, which is defined as:

$$sgn(s) = \begin{cases} -1 \; if \; s < 0 \\ 0 \; if \; s = 0 \\ 1 \; if \; s > 0 \end{cases} \quad (22)$$

If s_1 converges to zero, trivially x_e converges to zero. If s_2 converges to zero, in steady-state it becomes $\dot{\theta}_e = -\gamma_2 \cdot \theta_e - \gamma_0 \cdot sgn(\theta_e) \cdot |y_e|$. Since $|y_e|$ is always bounded, the following relationship between θ_e and $\dot{\theta}_e$ holds: $\theta_e < 0 \Rightarrow \dot{\theta}_e > 0$ and $\theta_e > 0 \Rightarrow \dot{\theta}_e < 0$.

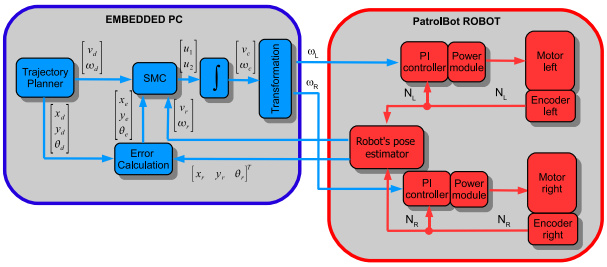

Fig. 3. Sliding-Mode Trajectory-Tracking control architecture.

The time derivative of (21) are

$$\begin{aligned} \dot{s}_1 &= \ddot{x}_e + \gamma_1 \cdot \dot{x}_e, \\ \dot{s}_2 &= \ddot{\theta}_e + \gamma_2 \cdot \dot{\theta}_e + \gamma_0 \cdot sgn(\theta_e) \cdot |\dot{y}_e|. \end{aligned} \quad (23)$$

Gao and Hung [15] proposed the method of reaching mode and reaching law, based on m-input n^{th}-order systems. In order to assure the attraction of state trajectory onto the switching manifold within the reaching mode, they suggested the control of reaching speed by certain reaching law. The general form of reaching law are

$$\begin{aligned} \dot{s} &= -Q \cdot s - P \cdot sgn(s) \quad (24) \\ Q &= diag\left[q_1, q_2\right], \quad q_i > 0, i = 1,2, \\ P &= diag\left[p_1, p_2\right], \quad p_i > 0, i = 1,2, \\ sgn(s) &= \left[sgn(s_1), sgn(s_2)\right]^T, \\ s &= \left[s_1, s_2\right]^T. \end{aligned}$$

Let us define $V = \frac{1}{2} \cdot s^T \cdot s$ as a Lyapunov function candidate, therefore its time derivative is

$$\begin{aligned} \dot{V} &= s_1 \cdot \dot{s}_1 + s_2 \cdot \dot{s}_2 = s_1 \cdot (-q_1 \cdot s_1 - p_1 \cdot sgn(s_1)) + \\ &+ s_2 \cdot (-q_2 \cdot s_2 - p_2 \cdot sgn(s_2)) = \\ &= -s^T \cdot Q \cdot s - p_1 \cdot |s_1| - p_2 \cdot |s_2|. \end{aligned}$$

For $\dot{V}$ to be negative semi-definite, it is sufficient to choose q_i and p_i such that $q_i, p_i \geq 0$.

Using a $sign$ function often causes chattering in practice. One solution is to introduce a boundary layer around the switch surface [16], [17]:

$$u_i = u_{eqi} - k_i \cdot sat\left(\frac{s_i}{\phi}\right), \; i = 1,2 \quad (25)$$

where constant factor ϕ defines the thickness of the boundary layer. $sat\left(s/\phi\right)$ is a saturation function that is defined as:

$$sat\left(\frac{s}{\phi}\right) = \begin{cases} \frac{s}{\phi} & if \quad \left|\frac{s}{\phi}\right| \leq 1 \\ sgn\left(\frac{s}{\phi}\right) & if \quad \left|\frac{s}{\phi}\right| > 1. \end{cases} \quad (26)$$

The equivalent control (u_{eqi}) can be interpreted as the continuous control law that would maintain $\dot{s} = 0$ if the dynamics were exactly known. From (7), (18) and (23) we can calculate the equivalent control

$$u_{eq1} = \frac{-D_1}{\alpha_{nom} \cdot cos\theta_e}, \quad u_{eq2} = \frac{-D_2}{\beta_{nom}}, \quad (27)$$

TABLE I

PARAMETER VALUES OF THE MOBILE ROBOT - PATROLBOT

Parameter	Value
mass of the robot body	46 kg
radius of the drive wheel	0.095 m
distance between wheels	0.480 m
moment of inertia	2.185 kgm^2
$\Delta\alpha_{max}$	0.033
$\Delta\beta_{max}$	0.12

where D_1 and D_2 are

$$D_1 = -\dot{x}\cdot\dot{\theta}_e\cdot sin\theta_d + \dot{y}\cdot\dot{\theta}_e\cdot cos\theta_d - \dot{\omega}_d\cdot y_e - \\ -\omega_d\cdot\dot{y}_e - \gamma_1\cdot\dot{x}_e, \\ D_2 = \dot{\omega}_d - \gamma_2\cdot\dot{\theta}_e - \gamma_0\cdot sgn(\theta_e)\cdot\dot{y}_e\cdot sgn(y_e). \tag{28}$$

Using (7), (21), (24) and (25) we can calculate

$$k_1 = \frac{Q_1\cdot s_1 + P_1\cdot sat(s_1/\phi) - D_1\cdot\frac{\Delta\alpha_{max}}{\alpha_{nom}}}{(\alpha_{nom}+\Delta\alpha_{max})\cdot cos\theta_e}, \\ k_2 = \frac{Q_2\cdot s_2 + P_2\cdot sat(s_2/\phi) - D_2\cdot\frac{\Delta\beta_{max}}{\beta_{nom}}}{(\beta_{nom}+\Delta\beta_{max})}. \tag{29}$$

IV. CLOSED-LOOP, REAL-TIME CONTROL RESULTS

To show the effectiveness of the proposed sliding mode control law numerically, real experiments were carried out on the trajectory-tracking problem of a nonholonomic wheeled mobile robot. The mobile robot is assumed to have the same structure as in Fig. 1. For obtaining the dynamic equation, parameter values of the mobile robot are given in Table I. The parameters of sliding modes were held constant during the experiments: $Q_1 = 1.5$, $Q_2 = 0.75$, $P_1 = 0.5$, $P_2 = 0.5$ and $\gamma_1 = 0.75$, $\gamma_2 = 2.5$, $\gamma_0 = 4.5$.

The robot has two-level control architecture (see Fig. 3). High-level control algorithms (including desired motion generation) are written in C++ and run with a sampling time of Ts = 100 ms on a embedded PC, which also provides a user interface with real-time visualization and a simulation environment. Wheel velocity commands,

$$\omega_R = \frac{v_c + L\cdot\omega_c}{R}, \quad \omega_L = \frac{v_c - L\cdot\omega_c}{R}, \tag{30}$$

are sent to the PI controllers, and encoder measures N_R and N_L are received in the robots pose estimator for odometric computations.

The real-time experiments are carried out on PatrolBot, a general purpose mobile robot acquired from MobileRobots Inc (see Fig. 4).

A. Mobile Platform - PatrolBot, Technical Specifications

PatrolBot is a programmable autonomous general purpose Service robot rover built by MobileRobots Inc [18].

PatrolBot has a 59cm x 48cm x 38cm, CNC aluminum body. Its 19 cm diameter tires handle nearly any indoor surface. The two motor shafts hold 1000-tick encoders. This differential drive platform is holonomic so it can turn in place. Moving wheels on one side only, it forms a circle

Fig. 4. The experimental mobile robot - PatrolBot.

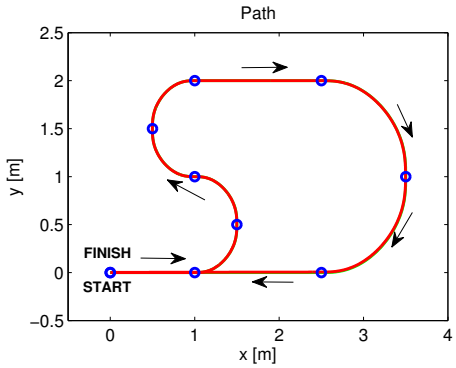

Fig. 5. Trajectory example to be tracked.

of 29 cm radius. The robot is equipped with 1.6 GHz Intel Pentium processor and 500 MB of RAM.

Software Specifications

A small proprietary μARCS transfers sonar readings, motor encoder information and other I/O via packets from the micro controller server to the PC client and returns control commands. PatrolBot can be run from the client or users can design their own programs under Linux or under WIN32 using C/C++ compiler. ARIA and ARNL software supply library functions to handle navigation, path planning, obstacle avoidance and many other robotic tasks.

B. Closed-loop Control Results

The real-time experiments was made for one type of trajectory shown in Fig. 5. Two types of experiments were made: A) without additional mass and B) with additional mass ($\approx$ 3 kg). Four experimental trials were executed for each type of experiments. In all cases the experimental data are summarized in Table II.

The trajectory-tracking must perform not only the planning of the curve (spatial dimension) but also the speed profile (temporal dimension). All the experiments had the expected results: the lateral, longitudinal and orientation errors that tends to zero with or without additional mass. The trajectories shown in Fig. 5 was obtained using the algorithm presented in [12]. In the case of trajectory-tracking the path is to be followed under time constraints. The trajectory has

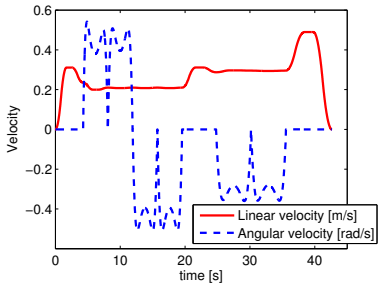

Fig. 6. Linear and angular velocities for trajectory depicted in Fig. 5.

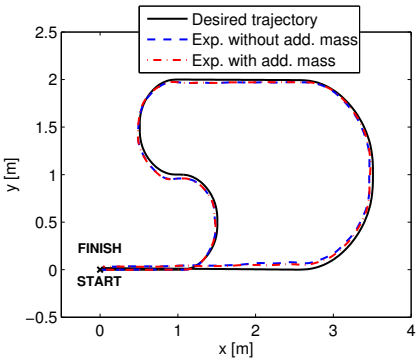

Fig. 7. Trajectories resulted after the experiments.

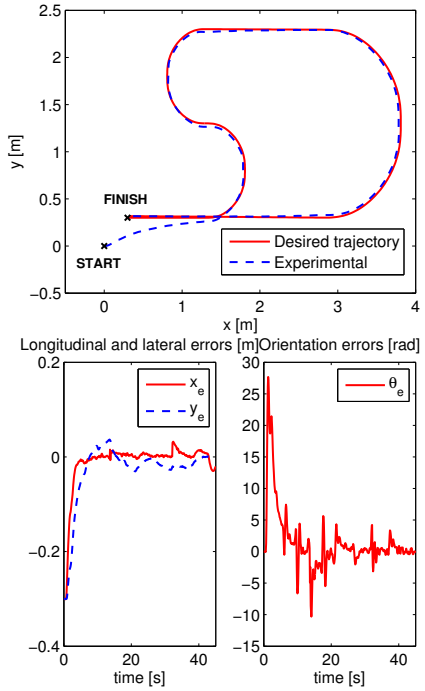

Fig. 9. Experimental control starting from an initial error state ($x_e = 0.3$, $y_e = 0.3$, $\theta_e = 0.0$).

an associated velocity profile (see Fig. 6), with each point of the trajectory embedding spatio-temporal information that is to be satisfied by the robot along the trajectory.

Fig. 7 presents the experiments using the PatrolBot robot with and without additional mass in case of trajectory shown in Fig. 5. From this figures we can observe that our sliding-mode trajectory-tracking controller is robustness with respect to system uncertainties. Fig 8 shows desired, command and real linear velocities for SM-TT control in case of trajectory-tracking without additional mass.

As shown in Fig. 9 the PatrolBot robot retrieved quickly ($\Delta_t \approx 10s$) and smoothly from its initial state error ($x_e = 0.30$, $y_e = 0.30$, $\theta_e = 0.00$), and the tracking errors converge on average to zero with acceptable reduced values along the trajectory.

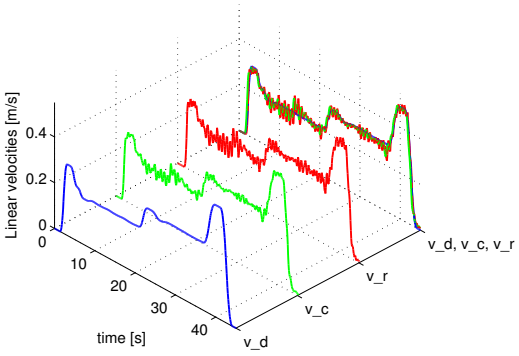

Fig. 8. Desired (v_d), command (v_c) and real (v_r) linear velocities for SM-TT control.

In Table II are represented the eight experiments using sliding-mode trajectory-tracking controller for PatrolBot robot. Four experimental trials were executed for each cases (with and without additional mass). The table shows the maximum (Max) and root mean square (RMS). The maximum absolute values of lateral and longitudinal errors are under $0.08\ m$ and the maximum absolute values of orientation error is under $12\ deg$. Root mean square error is an old, proven measure of control and quality. RMS can be expressed as $RMS = \left[\frac{1}{N}\sum x^2(i)\right]^{\frac{1}{2}}$.

V. CONCLUSIONS

This paper addressed the problem of tracking control around a desired trajectory, taking into account the dynamics of the vehicle, for wheeled mobile robots. The proposed solution is based on the sliding-mode approach. The main advantages of using sliding-mode control include fast response, good transient and robustness with respect to system uncertainties and external disturbances.

The experimental tests presented in this paper are representative of the average performance of the controllers. We had summarized our acquired experience in general observations that can be useful guidelines for implementation of the same control strategies in other type of mobile robots.

REFERENCES

[1] I. Kolmanovsky and N.H. McClamroch, "Developments in Nonholonomic Control Problems", *IEEE Control System*, vol. 15(6), 1995, pp. 20-36.

TABLE II

REAL-TIME RESULTS

Case	No	x_e Max $[m]$	x_e RMS	y_e Max $[m]$	y_e RMS	θ_e Max $[deg]$	θ_e RMS
A	I	0.0311	0.0072	0.0588	0.0276	7.4622	0.0438
	II	0.0336	0.0071	0.0672	0.0301	9.5197	0.0444
	III	0.0309	0.0072	0.0683	0.0286	11.2449	0.0457
	IV	0.0300	0.0072	0.0676	0.0269	11.9794	0.0450
B	I	0.0273	0.0078	0.0634	0.0293	8.2300	0.0412
	II	0.0322	0.0081	0.0778	0.0323	8.7290	0.0468
	III	0.0295	0.0084	0.0712	0.0281	8.9227	0.0453
	IV	0.0341	0.0082	0.0628	0.0283	7.2193	0.0424

[2] A.M. Bloch and M. Reyhanoglu, "Controllability and Stabilizability Properties of a Nonholonomic Control System", *In Proceedings of the 29th IEEE Conference on Decision and Control*, Honolulu, USA, 1990, pp. 1312- 1314.

[3] B. Andrea-Novel B, G. Camption and G. Bastin, "Control of Nonholonomic Wheeled Mobile Robots by State Feedback Linearization". *The International Journal of Robotic Research*, vol. 14(6), 1995, pp. 543-559.

[4] H.S. Shim and Y.G. Sung, "Stability and Four-posture Control for Nonholonomic Mobile Robots". *IEEE Transactions on Robotics and Automation*, vol. 20(1), 2004, pp. 148-154.

[5] A. Tayebi, M. Tadjine and A. Rachid, "Invariant Manifold Approach for the Stabilization of Nonholonomic Systems in Ehained Form: Application to a Car-Like Mobile Robot", *In Proceedings of the 36th IEEE Conference on Decision and Control*, San Diego, USA, 1997, pp. 4038-4043.

[6] A. Filipescu, U. Nunes and S. Stamatescu. "Discrete-Time Sliding-Mode WMR Control Based on Parameter Identification" , *in Proc. of the 16th IFAC World Congress*, Prague, 2005.

[7] J-H. Li and S-A. Wang, "Adaptive Trajectory Tracking Control of Wheeled Mobile Robots with Nonholonomic Constraint", *Journal of Electronic Science and Technology of China*, vol. 3(4), 2005, pp. 342-347.

[8] R. Fierro and F.L. Lewis, "Control of a Nonholonomic Mobile Robot: Backstepping Kinematics into Dynamics", *Journal of Robotic Systems*, vol. 14(3), 1997, pp. 149163.

[9] D. Chwa, "Sliding-mode Tracking Control of Nonholonomic Wheeled Mobile Robots in Polar Coordinates", *IEEE Transactions on Control Systems Technology*, 12(4), pp. 637–644, 2004.

[10] J. M. Yang and J. H. Kim. "Sliding Mode Control for Trajectory Tracking of Nonholonomic Wheeled Mobile Robots", *IEEE Transactions on Robotics and Automation*, 15(3), pp. 578–587, 1999.

[11] D. Chwa, S. K. Hong and B. Song, "Robust Posture Stabilization of Wheeled Mobile Robots in Polar Coordinates", *The 17th International Symposium on Mathematical Theory of Networks and Systems*, pp. 343-348, 2006.

[12] R. Solea and U. Nunes, "Trajectory Planning and Sliding-mode Control Based Trajectory-tracking for Cybercars", *Integrated Computer-Aided Engineering*, IOS Press, 14(1), pp. 33–47, 2007.

[13] W. E. Dixon, Z. P. Jiang and D. M. Dawson, "Global Exponential Setpoint Control of Wheeled Mobile Robots: a Lyapunov Approach", *Automatica*, 36, pp. 1741–1746, 2000.

[14] T. Floquet, J. P. Barbot and W. Perruquetti, "Higher-order Sliding Mode Stabilization for a Class of Nonholonomic Perturbed Systems", *Automatica*, 39, pp. 1077–1083, 2003.

[15] W. Gao and J. C. Hung, "Variable Structure Control of Nonlinear Systems: A New Approach", *IEEE Transactions on Industrial Electronics*, 40(1), pp. 45–55, 1993.

[16] J.J. Slotine and S.S. Sastry, "Tracking Control of Non-linear Systems Using Sliding Surfaces, With Application to Robot Manipulators", *Massachusetts Institute of Technology*, Cambridge MA 02139, Tehnical Report LIDS-P-1264, 1982, pp. 1-54.

[17] J.J. Slotine and W. Li, *Applied Nonlinear Control*, Prentice-Hall, Inc, Inglewood Cliffs, New Jersey, 1991.

[18] *ActivMedia Robotics*. Mobile robots. http://mobilerobots.com/.